Theoretical study of the structure and tautomerism of N^1-unsubstituted pyrazoles in the solid state

José Luis G. de Paz,*[,a] José Elguero,*[,b] Concepción Foces-Foces,[c] Antonio L. Llamas-Saiz,[c] Francisco Aguilar-Parrilla,[d] Olivier Klein[d] and Hans-Heinrich Limbach[d]

[a] *Departamento de Química Física Aplicada, Universidad Autónoma de Madrid, E-28049 Madrid, Spain*
[b] *Instituto de Química Médica, CSIC, Juan de la Cierva 3, E-28006 Madrid, Spain*
[c] *Departamento de Cristalografía, Instituto de Química Física 'Rocasolano', Serrano 119, E-28006 Madrid, Spain*
[d] *Institut für Organische Chemie (WE 02), Fachbereich Chemie, Freie Universität Berlin, Takustraße 3, D-14195 Berlin, Germany*

Ab initio **theoretical calculations have been performed on the pyrazole cyclic dimer, trimer and tetramers as well as on linear oligomers, assuming that there is no relaxation of the geometry during the proton transfer. The ground state and a wide variety of transition states, corresponding to different pathways for intermolecular proton transfer, have been explored and the results compared with experimental data from crystallography and solid state NMR spectroscopy. For the simplest case of the dimer, the reaction path corresponding to a double proton transfer has been explored as well as the effect of relaxing the geometry.**

Introduction

In a series of previous papers,[1–5] it has been shown by X-ray crystallography that certain N^1-unsubstituted pyrazoles form cyclic dimers, trimers or tetramers in the solid state, depending on the ring substitution pattern (Scheme 1). In these cyclic structures degenerate double, triple or quadruple proton transfers take place (Scheme 1) whose kinetics including some hydrogen–deuterium isotope effects have been followed by ^{15}N CPMAS NMR (CP, ^{1}H–^{15}N cross-polarization; MAS, magic angle spinning). Using *ab initio* calculations we have now explored the proton transfer reaction pathways of the three processes. The results of this study are reported in this paper (together with some new experimental kinetic results).[6] It is shown that the multiple proton transfer may be concerted or stepwise depending on the number of protons transferred and on whether one allows for major heavy atoms motions or not (this possibility has been explored only for the dimer).

Experimental results

Owing to annular tautomerism,[7] pyrazoles can exist in two tautomeric forms, N^1-unsubstituted, 3-R^3 and N^1-unsubstituted, 5-R^3, eqn. (1).

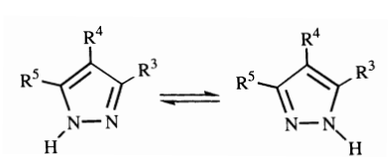

(1)

If R^3 ≠ R^5, four situations are possible in the solid state: (*i*) the most common is that where only one tautomer is present in the crystal and only one kind of crystal can be obtained; (*ii*) both tautomers are present in the crystal; (*iii*) two or, eventually, more polymorphs of the same tautomer can be isolated, and (*iv*) both tautomers crystallize in different crystal types (desmotropy). All these situations have been found in N^1-unsubstituted pyrazole compounds.[1–6]

Another important aspect for proton transfer concerns the hydrogen bond network formed by N^1-unsubstituted pyrazoles. The information available regarding simple compounds (that is, excluding pyrazoles bearing functional groups able to form supplementary hydrogen bonds) is summarized in Table 1.

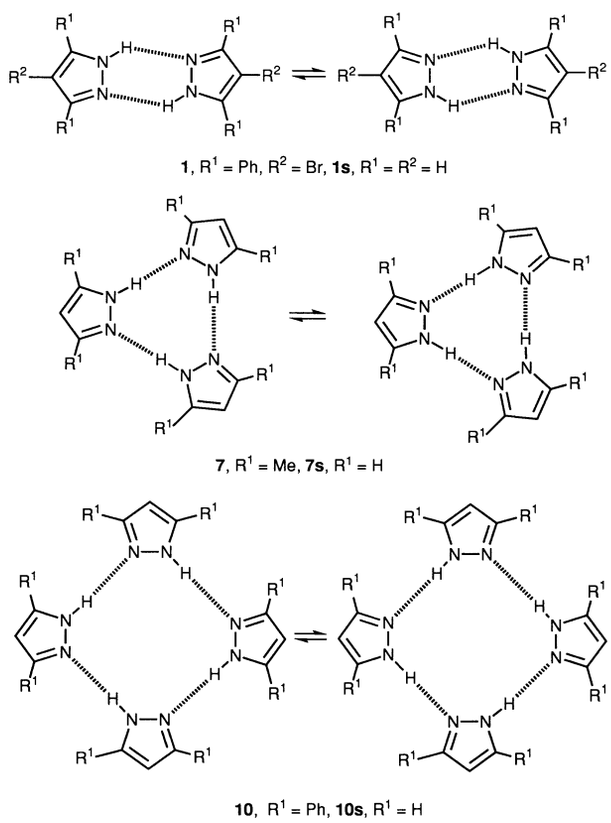

1, R^1 = Ph, R^2 = Br, **1s**, R^1 = R^2 = H

7, R^1 = Me, **7s**, R^1 = H

10, R^1 = Ph, **10s**, R^1 = H

Scheme 1

The X-ray structure of the pyrazoles of Table 1 can be found in the following references: **1**,[3] **2**,[8] **3**,[9] **4**,[9] **5** (desmotropy, **5a** and **5b**),[10] **6**,[9] **7**,[1,2] **8**,[4] **9**,[11] **10**,[12] **11**,[3,9] **12** [which presents polymorphism; one of the polymorphs corresponds to case (*ii*) and the

Table 1 Structure of simple N^1-unsubstituted pyrazoles in the solid state

	$R^3 = R^5$	$R^3 \neq R^5$
Cyclic dimers	**1**, $R^3 = R^5$ = Ph, R^4 = Br **2**, $R^3 = R^5 = Bu^t$, R^4 = H **3**, $R^3 = R^5 = Bu^t$, $R^4 = NO_2$ **4**, $R^3 = R^5$ = Ph, $R^4 = NO_2$	**5a**, R^3 = Me, $R^4 = NO_2$, R^5 = H
Cyclic trimers	**6**, $R^3 = R^5$ = H, $R^4 = NO_2$ **7**, $R^3 = R^5$ = Me, R^4 = H	**5b**, R^3 = H, $R^4 = NO_2$, R^5 = Me **8**, R^3 = Ph, R^4 = Br, R^5 = H **9**, $R^3 = CO_2Me$, $R^4 = CF_3$, R^5 = H **10**, Campho[*c*]pyrazole
Cyclic tetramers	**11**, $R^3 = R^5$ = Ph, R^4 = H	**12**, R^3 = Ph(Me), R^4 = H, R^5 = Me(Ph) (both tautomers, **12a** and **12b**)
Catamers[a]	**13**, $R^3 = R^4 = R^5$ = H **14**, $R^3 = R^5$ = Me, R^4 = Br **15**, $R^3 = R^5$ = Me, $R^4 = NO_2$	**16**, $R^3 = N_3$, R^4 = Ph, R^5 = H

[a] Catamer (from the Latin *catena* meaning 'chain'): a long chain of molecules held together by hydrogen bonds.

Table 2 Proton transfer in cyclic N^1-unsubstituted pyrazoles

Compound	Isotopic composition	log *A*	E_a/kcal mol^{-1}[a]	k/s^{-1} (330 K)	$k^{(H)n}/k^{(D)n}$	Contribution $\sqrt[n]{k^{(H)n}/k^{(D)n}}$
1, cyclic dimer	HH	11.4	10.6	6 400	k^{HH}/k^{DD} *ca.* 25	5
	DH	11.8	11.6			
	DD	13.4	15.1			
7, cyclic trimer	HHH	11.8	12.1	1 000	k^{HHH}/k^{DDD} *ca.* 50	3.68
	DHH	11.8	12.9			
	DDH	12.0	13.9			
	DDD	11.8	14.3			
10, cyclic tetramer	HHHH	11.8	10.6	11 300	k^{HHHH}/k^{DDDD} *ca.* 12	1.86
	DDDD	13.8	14.8			

[a] 1 kJ = 4.184 kcal.

other corresponds to tautomer **12a**, 3-phenyl-5-methylpyrazole],[13] **13**,[14,15] **14**,[16] **15**[17] and **16**.[18]

Proton transfer takes place only when cyclic structures are formed. It appears that the transfer of a large number of protons, present for example in catamers, requires a very high activation energy. In this work, we consider the case of compounds **1** (a cyclic dimer), **7** (a cyclic trimer), and **10** (a cyclic tetramer) as model compounds for the three cyclic structures. Other model compounds are **8**, formed by three 3-phenyl-4-bromopyrazole tautomers, which is a non-planar cyclic trimer with the *N*H proton localized, and pyrazole itself **13** forming a 'figure of eight' shaped catamer.

The information on compounds **1**, **7** and **10** came from crystallography (two, three and four 'half-protons' respectively) and from ^{13}C and, in particular, ^{15}N CPMAS–NMR spectroscopy. Variable temperature experiments provide activation energies and the use of deuteriated derivatives replacing *N*H by *N*D allowed us to determine the mechanism of the proton transfer by measuring the multiple isotope effects. The three model compounds mentioned previously are represented in Scheme 1, the kinetic results of the NMR study being reported in Table 2. The last column of Table 2 corresponds to the contribution calculated by the *n*-root of the ratio k^{Hn}/k^{Dn}.† Although a detailed analysis of the kinetic isotope effects has not yet been made, the data reported in Table 2 and, especially, the isotopic effects [19] suggest that in the case of the dimer **1** and the trimer **7** two and three protons respectively are in motion in the rate-limiting step; moreover in the case of the trimer a thermally activated tunneling process is present at low temperatures.[20] In the case of proton transfer of the tetramer **10**, the smaller isotope effects suggest a stepwise mechanism with two protons in motion in each step.[6]

† Table 2 present unpublished results by H.-H. Limbach, F. Aguilar-Parrilla, O. Klein and Ph. Lorente. $\sqrt[n]{k^{Hn}/k^{Dn}} = k^{H1Dm}/k^{HI-1Dm+1}$ represents the contribution of a single site assuming the validity of the rule of the geometric mean, valid in approximation in the case of a concerted multiple proton transfer process.

Computational details

All the calculations were carried out using the supercomputing facilities of the IBM Kingston Scientific and Engineering Department on a LCAP-3090 computer.[21,22] Theoretical calculations were performed using the programs (*i*) KGNMOL using its 'Add' option to save computational time in calculating the basis set superposition error (BSSE) and the energy of a fixed structure with a few atoms moving[23] and (*ii*) HONDO8 using C_{2v}, D_{2h}, C_{3v}, D_{3h}, D_{2d} and S_4 symmetries when necessary to save computational time.[24] Some preliminary calculations were performed at CC/UAM using the programs GAUSSIAN86[25] and HONDO7[24] on a 3090/VEC single cpu computer.

The standard basis sets of Pople,[26] Van Duijneveldt,[27] Clementi [21,22,28] and Dunning were used.[29] In particular, we have used Pople's STO-3G, 3-21G and 6-31G bases, Van Duijneveldt's [7,3/2,1], [9,5/4,2] and [11,7/4,2] bases, Dunning's [9,5/3,2] base and Clementi's GEOMEDIUM geometrical basis set, which is of double zeta quality. Polarization functions were added to C, N and H atoms on 6-31G, [9,5/3,2], [9,5/4,2] and GEOMEDIUM bases, first with standard Pople's exponents (0.8 for C and N atoms and 1.1 for H atoms) and then with the exponent corresponding to geometrical basis sets (0.324 for C, N and H atoms).

BSSE were evaluated using the Boys and Bernardi's counterpoise procedure[30] as is usual in the literature.[31,32] In most cases, this method is adequate and provides interaction energies in good agreement with those from larger basis sets.[31] Because we were trying to reproduce the behaviour of pyrazole crystals, most of the calculations were performed on geometries derived from experimental X-ray structures of compounds **1**, **7** and **10**. These geometries, which we will call 'simplified geometries' **1s**, **7s** and **10s**, are represented in Scheme 1. The dimer **1s** is almost perfectly planar and has a C_2 symmetry axis; the trimer **7s** is planar showing a C_{3h} symmetry and, finally, the tetramer **10s** has near a S_4 symmetry (in the dimer, trimer and tetramer only the *N*-H protons depart from these symmetries) and a structure which is far from planarity. They were obtained by replacing the

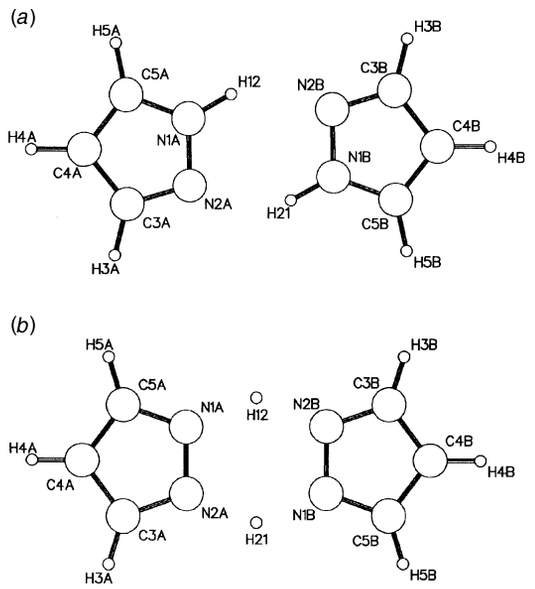

Fig. 1 Dimer: (*a*) Ground State, DGS; (*b*) Concerted Transition State, DCTS

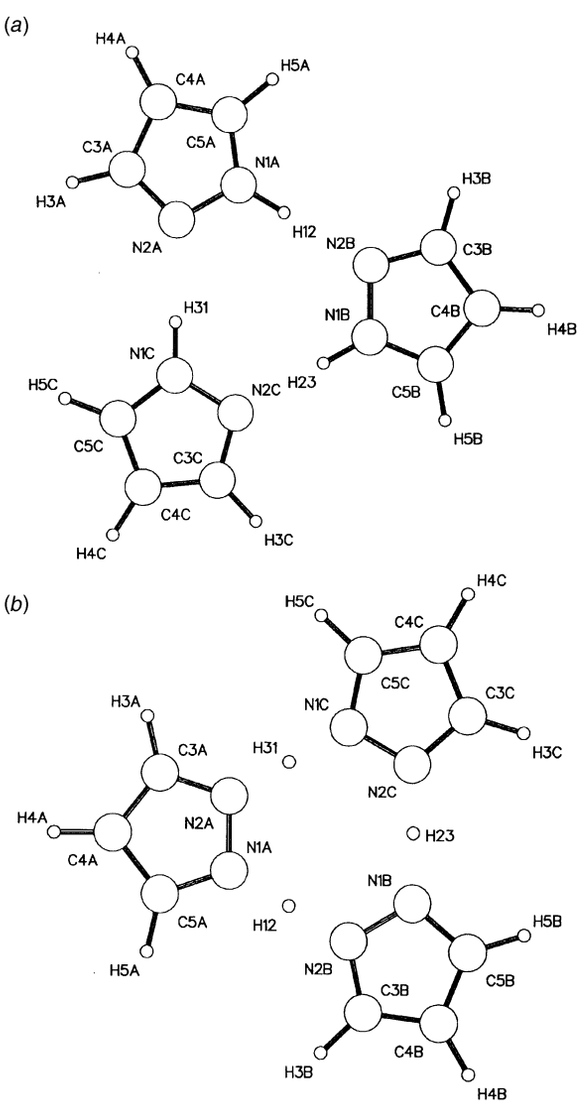

Fig. 2 Trimer: (*a*) Ground State, TrGS; (*b*) Concerted Transition State, TrCTS

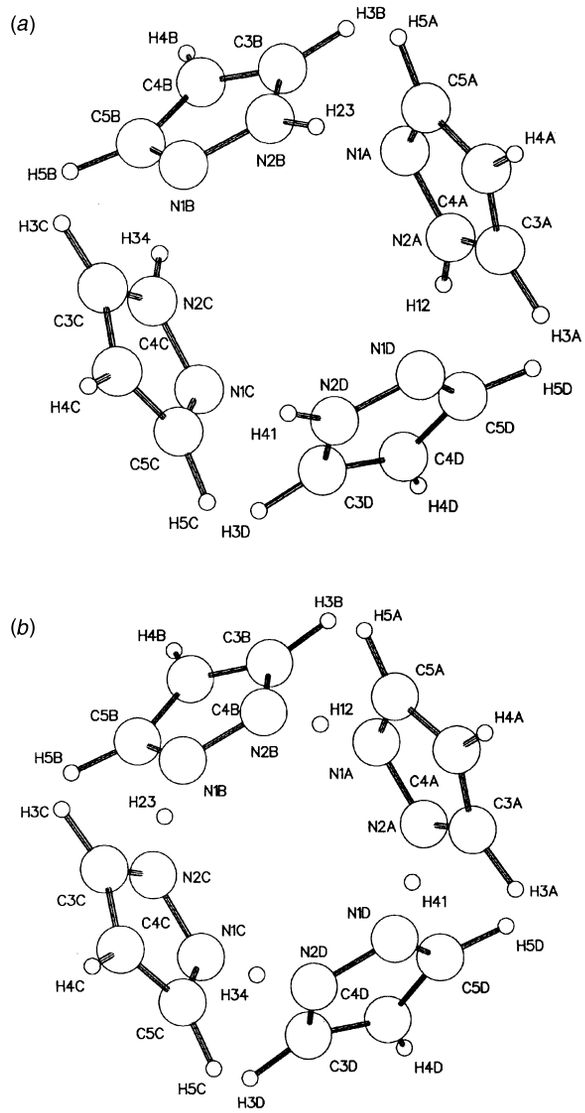

Fig. 3 Tetramer: (*a*) Ground State, TeGS; (*b*) Concerted Transition State, TeCTS

substituents by H atoms situated at 1.065 Å and with H–C–X angles taken from the 6-31G optimized geometry of pyrazole.[33]

The simplified structure of 3-phenyl-4-bromopyrazole **8s** by replacing the phenyl and bromo substituents by H atoms, and the structure of pyrazole itself **13** were used for calculations of cyclic trimers with localized protons in the ground state, and for catamers respectively (up to hexamers). Some representative geometries are represented in Fig. 1(*a*) (**1s**, dimer ground state, DGS, C_{2h} symmetry), 1(*b*) (**1s**, dimer concerted transition state, DCTS, D_{2h} symmetry), 2(*a*) (**8s**, trimer ground state, TrGS, C_{3h} symmetry), 2(*b*) (**7s**, trimer concerted transition state, TrCTS, D_{3h} symmetry), 3(*a*) (**10s**, tetramer ground state, TeGS, S_4 symmetry) and 3(*b*) (**10s**, tetramer concerted transition state, TeCTS, D_{2d} symmetry). DCTS, TrCTS and TeCTS are structures that, due to their point group symmetries, correspond to energy maxima (hill tops).

Relaxation of the geometry was performed in some cases using the HONDO and GAUSSIAN86 programs with appropriate gradient methods.[34,35] Due to the size of the systems under study, Dunning split-valence basis sets were used for geometry optimization. Correlation energies were calculated at the MP2 level of the theory[36] as well as using the Perdew–Zunger density functional,[37] which computes gradients of the electronic density and is implemented in the KGNMOL program. Density function methods were used to compute the correlation energy which was added to the HF energy.

Table 3 Pyrazole cyclic dimer (experimental X-ray geometry **1s**). Energies in Hartrees[a] and differences in energy in kcal mol^{-1}

	No. of basis set functions	ΔE_{SCF}	ΔE_{SCF} BSSE	ΔE_{MP2}	ΔE_{MP2} BSSE	DE PZ funct. BSSE	$E(a–b)$ SCF	$E(a–b)$ MP2	$E(a–b)$ PZ funct. corr.
Minimal									
STO-3G	58	−9.84	−5.30	−12.98	−6.95	−9.1	−443.358 12	−444.433 82	−2.707
[7,3/2,1]	58	−13.88	−10.38	−19.03	−12.53	−14.8	−447.774 48	−448.318 82	−2.659
Split-valence									
3-21G	106	−15.33	−9.99	−20.96	−12.01	−14.4	−447.008 40	−447.989 47	−2.651
6-31G	106	−11.12	−9.68	−16.09	−11.99	−14.7	−449.334 94	−450.312 53	−2.644
[9,5/3,2]	106	−10.61	−9.51	−17.29	−11.86	−15.1	−449.394 75	−450.328 08	−2.640
Double-zeta									
[9,5/4,2]	116	−12.26	−8.47	−17.81	−10.17	−14.1	−449.238 63	−450.347 16	−2.644
[11,7/4,2]	116	−10.41	−9.05	−14.81	−11.12	−14.7	−449.420 53	−450.543 57	−2.640
GEOMEDIUM	116	−9.68	−7.55	−15.03	−9.42	−13.2	−449.280 21	−450.404 29	−2.645
Split-valence + POL									
6-31G + (0.8,1.1)	190	−9.12	−7.62	−15.06	−11.19	−13.3	−449.551 47	−451.070 57	−2.647
6-31G + (0.324)	190	−9.70	−6.77	−19.02	−11.56	−13.0	−449.448 07	−450.773 22	−2.654
[9,5/3,2] + (0.8,1.1)	190	−8.37	−7.38	−15.75	−11.03	−12.4	−449.626 08	−451.104 57	−2.643
[9,5/3,2] + (0.324)	190	−9.28	−6.72	−19.47	−11.65	−12.4	−449.511 81	−450.812 78	−2.642
Double-zeta + POL									
[9,5/4,2] + (0.8,1.1)	200	−10.10	−6.38	−17.07	−9.43	−12.6	−449.529 29	−451.154 53	−2.645
[9,5/4,2] + (0.324)	200	−11.40	−6.45	−21.60	−11.11	−11.5	−449.482 46	−450.952 08	−2.638
GEOMEDIUM + (0.8,1.1)	200	−8.35	−6.16	−14.68	−9.32	−11.8	−449.563 56	−451.195 17	−2.646
GEOMEDIUM + (0.324)	200	−11.18	−6.63	−20.92	−11.24	−11.6	−449.472 05	−450.944 90	−2.647
GEOMEDIUM + (0.324)[b]	200	−12.24	−7.56	−22.02	−12.18	−12.6	−449.493 12	−450.966 00	−2.559

[a] Hartree = 627.503 kcal mol^{-1}. [b] Planar geometry.

Results and discussion

We discuss first the ground state geometries of the three compounds with the *N*H proton localized on one of the nitrogen atoms (for instance, left side formulae of Scheme 1). In the simplest case of the dimer **1s**, a more systematic exploration of the basis sets influence was carried out. Subsequently we describe the reaction pathways of the proton transfer following the information of Table 2: first, the barrier for the different pathways (concerted *vs.* stepwise) followed, in the case of the dimer, by (*i*) an exploration of the energy hypersurface and (*ii*) a study of the effect of geometry relaxaton.

Thermodynamic aspects: the ground state

Studies on the dimer. The results concerning the dimer **1s**, are reported in Table 3. Unless otherwise indicated, the calculations correspond to the simplified experimental geometry, obtained from the crystal structure. The two pyrazole molecules are designated by the letters *a* and *b*; consequently the dimer is referred to *a*–*b*. In the calculations $a–b_0$ is formed by monomer *a* plus the *b* ghost and $a_0–b$ by monomer *b* plus the *a* ghost.

The different columns of Table 3 have the following meaning: (*i*) number of basis set functions; (*ii*) $\Delta E_{SCF} = E_{SCF}\ (a–b) - (E_{SFC}\ a + E_{SCF}\ b)$ in the experimental structure a symmetry centre is absent and for this reason *a* and *b* are slightly different; (*iii*) ΔE_{SCF} BSSE $= E_{SCF}\ (a–b) - [E_{SCF}\ (a–b_0) + E_{SCF}\ (a_0–b)]$ (a_0 and b_0 are ghosts); (*iv*) $\Delta E_{MP2} = E_{MP2}\ (a–b) - (E_{MP2}\ a + E_{MP2}\ b)$; (*v*) ΔE_{MP2} BSSE $= E_{MP2}\ (a–b) - [E_{MP2}\ (a–b_0) + E_{MP2}\ (a_0–b)]$; (*vi*) ΔE_{funct} BSSE $= E_{SCF}$ BSSE $+ [E_{funct}(a–b) - E_{funct}(a–b_0) - E_{funct}\ (a_0–b)]$; (*vii*) $E\ (a–b)_{SCF}$ = SCF energy of the dimer; (*viii*) $E\ (a–b)_{MP2}$ = energy of the dimer at the MP2 level; (*ix*) $E\ (a–b)_{funct.corr.}$ = density functional correction of the SCF energy of the dimer *a*–*b*). The last row of Table 3 corresponds to the planar geometry, its energy being 13.2 kcal mol^{-1} lower than that of the corresponding non-planar experimental geometry (this geometry is not perfectly centrosymmetric due to the NHs and has a residual dipole moment of μ *ca.* 0.3–0.4 D).

Correlation corrections were calculated using MP2 and Perdew–Zunger density functional theories. Although correlation corrections for minimal or non-polarized basis sets are meaningless, they were evaluated for comparative purposes. For our problem, the criterion of selection of the best basis set should not necessarily be the minimum absolute energy of the (*a*–*b*) dimer (Hartree–Fock limit) but the basis set which gives the better description of the dimer, which we will call a 'balanced basis set'. A possible criterion could be the basis set that minimizes the BSSE. From the whole data of Table 3, we may assume that $\Delta E_{(dimer)}$ *ca.* −12 kcal mol^{-1} is the 'best value'.

STO-3G performances are obviously very poor; the fact that the STO-3G value without BSSE correction (ΔE_{SCF} = −9.84 kcal mol^{-1}) is close to the best value is certainly due to cancelling of errors. Van Duijneveldt's [7,3/2,1] minimal basis sets, which were specially built for the calculation of interaction energies, performs much better (even when compared with the 3-21G basis set), not only for the absolute energies but for the stabilization energy ΔE_{SCF} + BSSE = −10.38 kcal mol^{-1}. In a parallel way, for split-valence basis sets, the Dunning [9,5/3,2] performs better than the 6-31G, also showing a lower value of BSSE.

The GEOMEDIUM basis set was optimized in atoms and was especially designed to minimise BSSE and to evaluate energy interactions at post-SCF level.[21,22,28] We added polarization functions to the best performing split-valence or double zeta basis sets. Diffuse polarization exponentials afford larger BSSE corrections and lower interaction energies both at SCF and at MP2 levels. MP2 values after BSSE correction show the excellent performances of geometrical basis sets like GEOMEDIUM plus geometrical exponent for polarization functions. Density functional theory (DFT) corrections also present larger BSSE corrections for diffuse exponent, but, on the whole, non expensive DFT and unsophisticated basis sets afford results in acceptable agreement with those obtained with larger basis sets.

Another factor to consider when selecting a basis set for this kind of calculations is the cpu time. As an example, a full MP2/[9,5/4,2] + pol (0.324) calculation of the experimental pyrazole dimer using the ADD option of KGNMOL for the calculation of the BSSE, takes about 7.0 h of cpu time and 2256 cylinders of an IBM 3380 DASD for storing one- and two-electron integrals. The same calculation for GEOMEDIUM + pol (0.324) takes 9.4 h and 2044 cylinders. A reasonable compromise is to use density functionals in the evaluation of the correlation correction or to impose a planar geometry for the dimer: consider the following cpu times in h for calculating the correlation correction [GEOMEDIUM + pol (0.324)]: SCF 4.7 and 2.5, MP2 2.8 and 1.9, density functional 1.4 and 1.5 (respectively, experimental and planar).

Table 4 Stabilization energies including BSSE (kcal mol^{-1}) in cyclic and linear N^1-unsubstituted pyrazoles, using experimental X-ray based geometries. (Note that the cyclic ones have an extra hydrogen bond compared with the linear ones)

	Minimal [7,3/2,1] including BSSE		Split-valence [9.5/3,2] including BSSE	
	Cyclic	Linear	Cyclic	Linear
Monomer	0	0	0	0
Dimer	−10.38	−5.04	−9.51	−4.26
Trimer	−23.65	−10.80	−19.51	−9.28
Tetramer	−42.10	−16.79	−34.20	−14.54
Hexamer	—	−29.05	—	—

In summary, at least a Dunning split-valence basis set including BSSE correction must be used to evaluate non-pairwise energies at SCF level. Reliable energies must include BSSE, correlation corrections and a DZP basis set. Geometrical basis sets, like GEOMEDIUM, could be a good choice taking into account the fact that they were specially designed for this kind of problem. For large systems, like the ones discussed in this paper, another acceptable possibility is to use Van Duijneveldt's [7,3/2,1] basis sets.

Cooperative effects. Brédas *et al*. have studied the electronic structure of hydrogen-bonded imidazole chains at the STO-3G and 4-31G levels.[38] Due to the position of its nitrogen atoms, imidazole cannot form cyclic structures, at least with a small number of monomers. Concerning the stabilization (STO-3G calculations), imidazole dimer [ΔE = dimer − 2(monomer)] is stabilized by 10.7 kcal mol^{-1}, which increases for the infinite chain up to 20.3 kcal mol^{-1}. Taking into account the BSSE correction, the dimer is 8.8 kcal mol^{-1} (STO-3G) and 9.9 kcal mol^{-1} (4-31G) more stable than the monomer.

In the case of pyrazole, the stabilization energies are reported in Table 4 with the same definition: $\Delta E = n$-mer − n(monomer). For the linear dimer, we obtain stabilization values of *ca.* 4–5 kcal mol^{-1}, half those of imidazole, while the cyclic dimer is much more similar to imidazole.

These energies increase with the number of hydrogen bonds, HBs: monomer HB = 0, linear dimer HB = 1, linear trimer HB = 2, linear tetramer HB = 3, linear hexamer HB = 5 (number of HBs = number of pyrazoles − 1); monomer HB = 0, $HB^2 = 0$, dimer HB = 2, $HB^2 = 4$, trimer HB = 3, $HB^2 = 9$, tetramer HB = 4, $HB^2 = 16$ (number of HBs = number of pyrazoles except for pz = 1, the isolated pyrazole monomer, where HB = 0).

The values of Table 4 correspond to eqns. (1)–(4).

$$\Delta E \text{ (linear, minimal)} = 0.5316 - 5.8489\ (n \text{ HBs}),\ 5 \text{ points}, \quad r^2 = 0.9987 \quad (1)$$

$$\Delta E \text{ (linear, split-valence)} = 0.276 - 4.864\ (n \text{ HBs}),\ 4 \text{ points}, \quad r^2 = 0.9978 \quad (2)$$

$$\Delta E \text{ (cyclic, minimal)} = 0.0652 - 2.6342\ (n \text{ HBs})^2,\ 4 \text{ points}, \quad r^2 = 0.999987 \quad (3)$$

$$\Delta E \text{ (cyclic, split-valence)} = -0.4424 - 2.119\ (n \text{ HBs})^2,\ 4 \text{ points}, \quad r^2 = 0.991 \quad (4)$$

There is no attenuation effect when n increases to the hexamer for linear catamers and to the tetramer for cyclic structures (the attenuation was observed by Brédas *et al*.[39] for imidazole trimer, since the value for the infinite chain is only twice the value of the dimer); it should appear in the case of pyrazoles for a much larger number of monomers.

The fact [eqns. (1) and (2)] that ΔE increases with the number of HBs for the catamers and [eqns. (3) and (4)] with the square of the number of HBs in the cyclic structures corresponds to the formation of two HBs for each pyrazole, since this molecule acts simultaneously as an acceptor and a donor of HBs.

Table 5 Differences in energies (kcal mol^{-1}) for the different transition states of the dimer **1c**, the trimer **7c**, and the tetramer **10c** corresponding to displacements of the proton between nitrogen atoms based on X-ray geometries

	Dimer **1c**[a]		
Basis set	DCTS	$D^{\pm}$	Structure **1**
SCF [9,5/3,2]	53.7	26.3	33.6
MP2/[9,5/3,2]	32.6	20.8	22.5
SCF/GEOMEDIUM + POL	53.4	29.2	35.2
MP2/GEOMEDIUM + POL	27.4	23.2	22.3
PZ[b]/GEOMEDIUM + POL	24.6	17.9	34.6
CC[c]/GEOMEDIUM + POL	55.3	29.2	36.2
SCF/[11,7/4,2]	51.8	25.6	33.2

	Trimer **7c**					
Basis set	TrCTS	$Tr^{\pm}$	Struct. **1**	Struct. **2**	Struct. **3**	Struct. **4**
SCF/[9,5/3,2]	28.3	32.3	21.0	21.4	36.0	40.3
PZ/[9,5/3,2]	25.8	31.0	20.4	—	34.1	39.7

	Tetramer **10c**			
Basis set[d]	TeCTS	$Te_{12}^{\pm}$	$Te_{13}^{\pm}$	Struct. **1**
SCF/[9,5/3,2]	72.3	25.1		26.7

[a] The optimized ground state (DGS) has C_{2h} symmetry. [b] Perdew–Zunger D.F. correlation correction. [c] Clementy–Chakavorty correlation correction. [d] 212 basis sets functions.

Dynamic aspects: the proton-transfer pathway

Structure and energy of the different transition states. For three cases, the dimer, trimer and tetramer, we have calculated the stationary points along the concerted reaction pathways where all mobile protons are in motion. We have also explored the stepwise pathways for the dimer, the trimer and the tetramer in a similar way as that used by Ahlberg and Truhlar in the case of amidine dimer and by Kim in the case of formic acid dimer.[39,40] The calculated stationary points are not necessarily saddle points, they can even be local minima; the structures DCTS, TrCTS and TeCTS, as explained before, are hill tops for symmetry reasons. In Schemes 2, 3 and 4, the stationary points

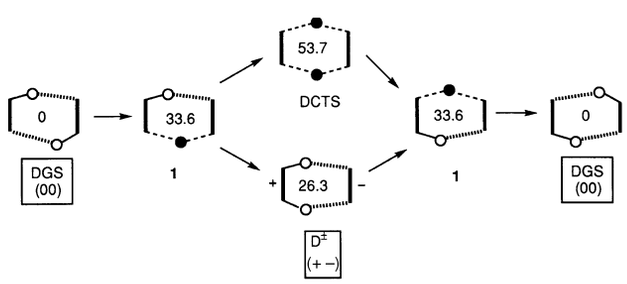

Scheme 2

of the dimer, trimer and tetramer are visualized as follows: a bold straight line represents a pyrazole ring, a plain line an N−H bond, an unfilled circle a proton bonded to a nitrogen atom, a filled circle a proton in motion between two pyrazoles. Thus, a normal HB will be represented by a series of small lines and, by contrast, when the proton is in the middle, it will be connected to nitrogen atoms by two broken lines. The ground states formed by neutral pyrazoles (pzH) are named (00) **1s**, (000) **7s** and (0000) **10s** while + and − signs denote charged pyrazolium cations (pzH_2, +) and pyrazolate anions (pz, −) respectively. The results of these calculations are gathered in Table 5, but to facilitate the discussion, inside each formula the relative value of the energy (in kcal mol^{-1}, corresponding to Dunning [9,5/3,2] calculation) has been added. Some structures corresponding to a complete transfer of a proton, *i.e.* the

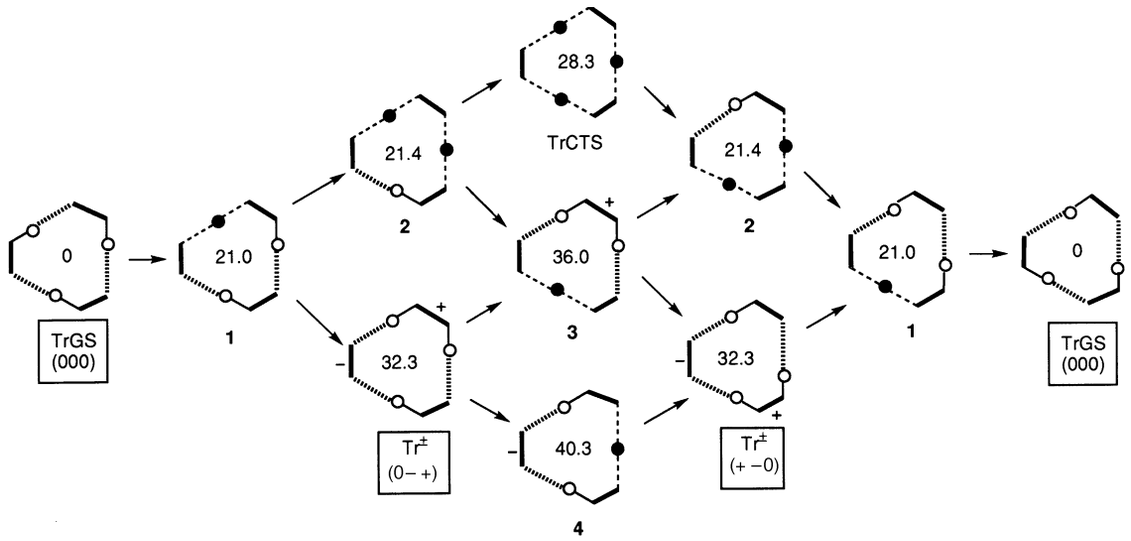

Scheme 3

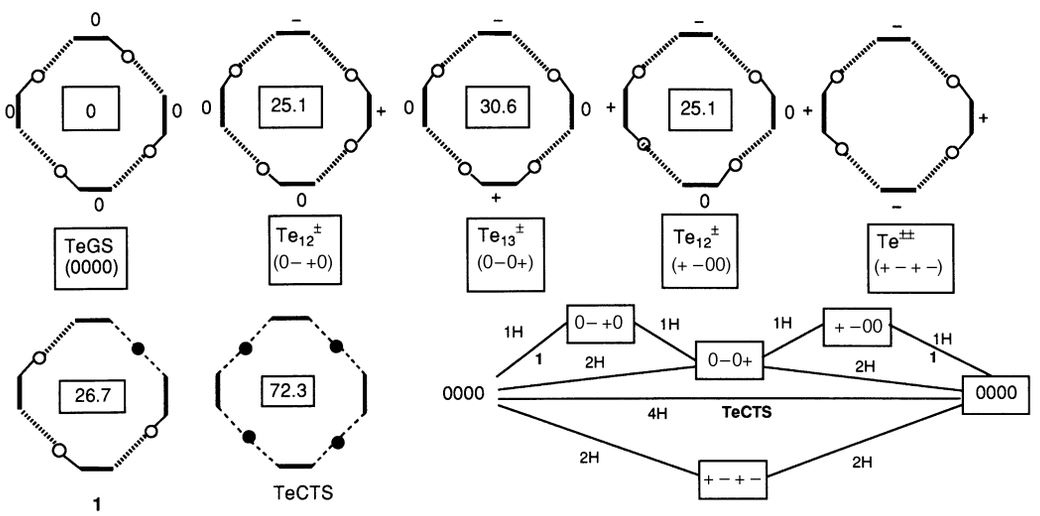

Scheme 4

presence of simultaneously a pyrazolium cation and a pyrazolate anion, have been marked by (D,Tr.Te)$^{\pm}$. The concerted mechanism would imply a single barrier connecting the potential wells (DGS, TrGS, TeGS) through the hill tops (DCTS, TrCTS, TeCTS).

For the same level of accuracy (Dunning [9,5/3,2] without relaxation of the geometry) the three profiles can be compared (Table 6).

In the case of the dimer, since it is easier to go through D$^{\pm}$ than through DCTS, the predicted pathway without relaxation of the geometry should be stepwise, while the experimental results are not yet clear but seem to point to a single barrier.[6] In the case of the trimer, the path through TrCTS is the lowest in energy, while the other paths must pass through barriers of 36.0 and 40.3 kcal mol^{-1}. Here the theory and the experiments are in good agreement.

The case of the tetramer **10s** is the most complex and, for this reason, Scheme 4 is a little different from the previous ones. The ground state is (0000) and the calculated intermediates are $Te_{12}^{\pm}$ (12 since the charged heterocycles are adjacent) and $Te_{13}^{\pm}$ (13 since the charged pyrazoliums are opposite). The intermediate $Te^{\pm\pm}$ was not calculated but two 'transition states', structure **1** [in the pathway between (0000) and (0− +0) and between (+ −00) and (0000)] and the hill top, TeCTS, were calculated.

Considering only structures with the protons at bond distances of the N atoms, Scheme 4 also shows that there are four ways to travel from (0000) to (0000) (degenerate intermolecular quadruple proton transfer): (*i*) a series of four 'one proton' jumps (0000) ⟶ (0− +0) ⟶ (0−0+) ⟶ (+ −00) ⟶ (0000); (*ii*) two series of two 'two proton' jumps (0000) ⟶ (0−0+) ⟶ (0000) and (0000) ⟶ (+ − + −) ⟶ (0000), and (*iii*) a 'four proton' jump (0000) ⟶ (0000). The concerted pathway (*iii*) costs considerably more energy than the stepwise mechanism though $Te_{12}^{\pm}$ and $Te_{13}^{\pm}$. The tetra-charged state, $Te^{\pm\pm}$, should be highly energetic, thus the lowest energy mechanism is the stepwise mechanism (0000) ⟶ (0−0+) ⟶ (0000) which agrees with the available experimental evidence.

For the three processes, the calculated values of ΔE are much higher than the experimental E_a values, roughly 2–2.5 times larger. Although the substituents are not the same for the calculated (C-unsubstituted pyrazoles) nor for the experimental results (C-substituted pyrazoles), we do not think that this could explain these differences which might arise from insufficiencies of the theoretical calculations.

Reaction path in the case of the dimer. We have calculated with GEOMEDIUM plus geometrical polarization functions, at the SCF and MP2 levels, 31 points of the energy hypersurface in the case of the planar dimer **1c**. These points have been situated in the way of the migration of the proton, considering two situations: (*i*) the other proton migrates simultaneously keeping the centre of symmetry; and (*ii*) the other proton remains in its initial position. Nevertheless, in these studies some other combinations were also explored.

To save computational time, we have carried out a series of

Table 6 Comparison theory–experiment for the proton transfer in pyrazole dimers, trimers and tetramers

Theory [9,5/3,2]				Experiment	
Type	Concerted	Stepwise	TS	Type	E_a
Dimer (Scheme 2)	53.7 (DCTS)	26.3 ($D^{\pm}$)	**33.6** (**1**)	Concerted	10.6
Trimer (Scheme 3)	**28.3** (TrCTS)	32.3 ($Tr^{\pm}$)	36.0 (**3**)	Concerted	11.8
Tetramer (Scheme 4)	72.3 (TeCTS)	**30.6** ($Te_{13}^{\pm}$)	26.7 (**1**)[a]	Stepwise	11.8

[a] This value corresponds to the TS between TeGS and $Te_{12}^{\pm}$; there should be a transition state of higher energy between $Te_{12}^{\pm}$ and $Te_{13}^{\pm}$.

calculations on the dimer **1c** with the following assumptions: the dimer, which is slightly non-planar and asymmetric, has been made planar and symmetrized by imposing a centre of symmetry; these assumptions we believe do not have significant influence on the results. Then, taking advantage of KGNMOL possibilities, without moving the distance between the pyrazole rings, a series of SCF and MP2 optimizations have been made for different positions of the two protons. Since the energy (see Table 9 of the Supplementary Material‡) depends on the position of both protons, the representation will require a five dimensional space. Consequently, we will discuss the data of Table 9 only in two cases: when a proton is kept fixed and the other is moved and when both move synchronously with regard to the symmetry centre.

The ground state corresponds to points 10 (coordinates ±0.52/±1.08) at the SCF level and near to point 18 (coordinates ±0.45/±1.08) at the MP2 level. By approaching the protons closer to the pyrazole ring (point 1) the value of ΔE rapidly increases.

The concerted mechanism, shown on the left side of Scheme 5, goes from point 10 to point 28 through the transition state

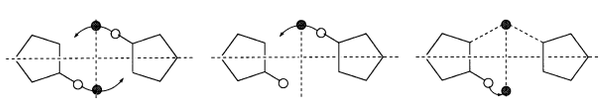

Scheme 5

DCTS and costs 55.2 kcal mol^{-1} at the SCF level and 29.5 kcal mol^{-1} at MP2 level. We have explored the geometry of the DCTS (points 23, 24, 28, 29, 30) and it appears that the proton follows a sinusoidal path (see Scheme 6).

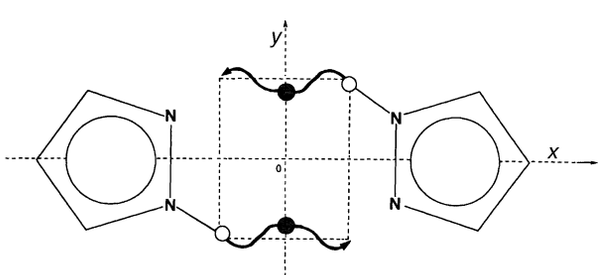

Scheme 6

The stepwise pathway (from GS to $D^{\pm}$, Scheme 5, middle), that is, from point 10 to points 13 or 20 represents an increase of 30 kcal mol^{-1} in energy (SCF) or 23 kcal mol^{-1} (MP2). Approaching the protons of the pyrazolium cation closer to the pyrazole ring (points 2 ≡ 31) increases the MP2 energy by 9–10 kcal mol^{-1}. The complete profile of the migration of the proton H2 from GS to $D^{\pm}$ has been calculated for two positions of proton H1 (X1 = 0.52 Å, points 11, 10, 9, 8, 6, 5, 4, 3, 2, and X1 = 0.42 Å, points 19, 18, 17, 16, 15, 14, 13, 12). Since they are very similar, only the case X1 = 0.52 Å is represented in Fig. 4. Two 'excursions' have been made, one from point 6 to point 7 and the other from point 19 to points 21 and 22. In both cases the energy increases.

Finally, we have explored the situation depicted on the right side of Scheme 6; *i.e.* how to reach the DCTS in a non-synchronous mechanism. When points 27, 26, 25, 28 are taken into account there is a regular increase in the energy (33, 36, 49, 55 kcal mol^{-1}, SCF, and 19, 19, 26, 29 kcal mol^{-1}, MP2).

In conclusion it appears that even the simplest case of pyrazole dimers the mechanism of the double proton transfer is rather complicated involving multidimensional pathways.

The problem of the relaxation of the geometry. Although this paper is devoted to the study of proton transfer without relaxation of the geometry, the importance of relaxation is well established for other (HNH) systems, such as $[H_3N\cdots H\cdots NH_3]^+$.[41] The closest example to pyrazole dimers is that of formamidine dimers studied by some of us.[42]

Table 7 Geometry (distance N···H···N between two adjacent pyrazole rings in Å) in the case of dimer **1s**

Compound	Experimental geometry	Calculated without relaxation	Calculated with relaxation
DGS	2.836[a]	2.945	—
DCTS	—	2.945	2.447
$D^{\pm}$	—	2.945	2.568
Structure **1**	—	2.945	2.814 (1 × N–H···N) 2.559 (1 × N···H···N)

[a] Average value in compound **8** (since the 3-phenyl-4-bromopyrazole dimer is not centrosymmetric there are two N···H···N distances, 2.828 and 2.845 Å).

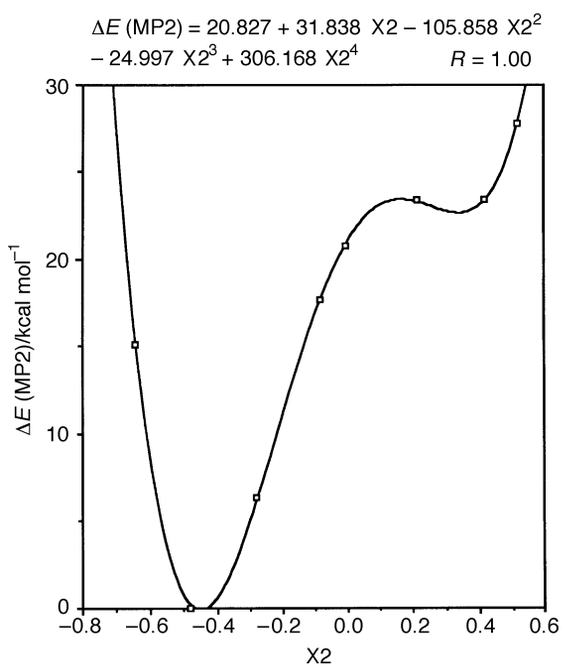

Fig. 4 Dimer proton transfer profile

‡ Tables 9–11 are available as supplementary data from the British Library (Supp. Pub. 57184, 5 pp.). For details of the British Library Publications scheme, see 'Instructions for Authors', *J. Chem. Soc., Perkin Trans. 2*, 1997, Issue 1.

Table 8 Summary of theoretical and experimental results (E highest energy along the reaction path; m number of protons in flight, n total number of protons transferred; g number of imaginary frequencies)

		Concerted			Stepwise			Experimental	
	n	E/kcal mol^{-1}	m	g	E/kcal mol^{-1}	m	g	Class	E_a/kcal mol^{-1}
Dimer	2	53.7 (**29.2**)	2	2	33.6	1	1	Concerted	10.6
Trimer	3	**28.3** (27.7)	3	1	36.0	1	1	Concerted	11.8
Tetramer	4	72.3 (35.7)	4	2	**26.7**	1	1	Stepwise	11.8

	Without geometry relaxation		With geometry relaxation		Experimental	
	Concerted	S	Concerted	S	Class	E_a/kcal mol^{-1}
Dimer	53.7	26.3	**29.2**	25.4	Concerted	10.6
Trimer	**28.3**	32.3	27.7	—	Concerted	11.8
Tetramer	72.3	**25.1**	35.7	—	Stepwise	11.8

The fact that the phenomena reported in the present paper occur in the solid state is irrelevant since the geometry changes will affect only high energy structures (transition states, saddle points, hill tops) very weakly populated. Experimental evidence that this is indeed the case is that activation energies for proton transfer in pyrazoles are about the same in the solid state (Table 2) and in solution (solvent assisted).[43]

In order to examine the effect of relaxation we have chosen the simplest case of dimer **1s**. At the same level of the theory (SCF/[9,5/3,2]) (see Table 5), the energy difference of DCTS (with regard to DGS) lowers from 53.7 to 29.2 kcal mol^{-1} (point group D_{2h}) and that of D$^{\pm}$ from 26.3 to 25.4 kcal mol^{-1} (point group C_{2v}).

The modification of the inter-pyrazole distances is significant: in Table 7 we have summarized the available information concerning the geometry; with regard to the optimized ground state GS, the shortening of the distance between pyrazole rings is very important (0.35 Å in average).

To represent the modification of the potential energy surface we have used those reported in ref. 42 for the degenerate intermolecular double proton transfer of formamidine (Fig. 5). r_1 and r_2 are the coordinates of the two protons (the values between 1.6 and −1.6 Å are arbitrary in our case); r_s, r_a and r_{as} represent, respectively, the coordinates of the transfer DGS ⟶ DCTS ⟶ DGS, D$^{\pm}$ ⟶ DCTS ⟶ D$^{\pm}$, DGS ⟶ D$^{\pm}$ ⟶ DGS. Without relaxation of the geometry [Fig. 5(*a*)], DCTS (hill top) lies much higher in energy than D$^{\pm}$ (27.4 kcal mol^{-1} higher) and although there is a transition state (saddle point) between DGS and D$^{\pm}$ (≤33.6 kcal mol^{-1}, Table 5, structure **1**, r_1 constant, is near this transition state) the pathway DGS ⟶ **1** ⟶ D$^{\pm}$ ⟶ **1** ⟶ DGS is much less energy demanding than going through the hill top DCTS (53.7 kcal mol^{-1}, Table 5). Relaxation of the geometry modifies considerably the potential energy surface [Fig. 5(*b*)] which becomes quite flat, making both pathways possible.

Since relaxing the geometry has almost no effect of D$^{\pm}$ we have calculated (SCF/[9,5/3,2]) only this effect for the relative energies (with regard to ground state) of TrCTS (27.7 kcal mol^{-1}, point group D_{3h}) and of TeCTS (35.7 kcal mol^{-1}, point group D_{2d}). For the trimer **7s** the effect is negligible while for the tetramer **10s** it is very important.

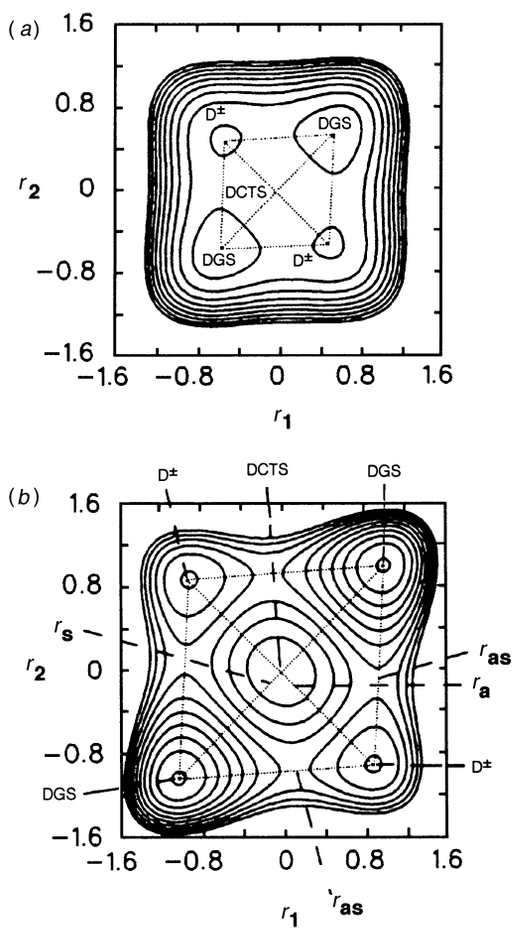

Fig. 5 Model potential energy surface for a degenerate intermolecular double proton transfer in pyrazole dimer **1s**

Conclusions

The main conclusions of this study are that to describe with some accuracy the problem of proton transfer in pyrazole crystals, even neglecting tunnelling effects, requires high level calculations and geometry relaxation. The image these calculations offer is summarized in Table 8.

Although these results are not entirely satisfactory, they provide for the first time a coherent view of proton transfer in cyclic n-mers of pyrazoles (n = 2, 3, 4).

Acknowledgements

This work was carried out at the IBM-Kingston Research Centre; Professor Enrico Clementi (now at the Université Louis Pasteur, Strasbourg, France) and Professor Gina Corongiu (now at the Centro Ricerca Sviluppo, Studi Superiori Sardegna, Cagliari, Italy) are gratefully acknowledged. The work was partly supported by the CYCIT of Spain and by the EC. One of us (J. L. G. D. P.) acknowledge the Spanish Ministry of Education for a grant and the IBM-Kingston Visiting Professor

Program for its help. This work is partly based on results from the MOTECC program (MOTECC is a trademark of IBM corp).

References

1 A. Baldy, J. Elguero, R. Faure, M. Pierrot and E. J. Vincent, *J. Am. Chem. Soc.*, 1985, **107**, 5290.
2 J. A. S. Smith, B. Wehrle, F. Aguilar-Parrilla, H.-H. Limbach, C. Foces-Foces, F. H. Cano, J. Elguero, A. Baldy, M. Pierrot, M. M. T. Khursid and J. B. Larcombe-McDouall, *J. Am. Chem. Soc.*, 1989, **111**, 7304.
3 F. Aguilar-Parrilla, G. Scherer, H.-H. Limbach, C. Foces-Foces, F. H. Cano, J. A. S. Smith, C. Toiron and J. Elguero, *J. Am. Chem. Soc.*, 1992, **114**, 9657.
4 F. Aguilar-Parrilla, C. Cativiela, M. D. Díaz de Villegas, J. Elguero, C. Foces-Foces, J. I. García, F. H. Cano, H.-H. Limbach, J. A. S. Smith and C. Toiron, *J. Chem. Soc., Perkin Trans. 2*, 1992, 1737.
5 J. Elguero, F. H. Cano, C. Foces-Foces, A. L. Llamas-Saiz, H.-H. Limbach, F. Aguilar-Parrilla, R. M. Claramunt and C. López, *J. Heterocycl. Chem.*, 1994, **31**, 695.
6 H.-H. Limbach, F. Aguilar-Parrilla, O. Klein, J. Elguero and N. Jagerovic, unpublished results.
7 J. Elguero, C. Marzin, A. R. Katritzky and P. Linda, *The Tautomerism of Heterocycles*, Academic Press, New York, 1976.
8 F. Aguilar-Parrilla, H.-H. Limbach, C. Foces-Foces, F. H. Cano, J. Elguero and N. Jagerovic, *J. Org. Chem.*, 1995, **60**, 1965.
9 A. L. Llamas-Saiz, C. Foces-Foces, F. H. Cano, P. Jiménez, J. Laynez, W. Meutermans, J. Elguero, H.-H. Limbach and F. Aguilar-Parrilla, *Acta Crystallogr., Sect. B*, 1994, **50**, 746.
10 C. Foces-Foces, A. L. Llamas-Saiz, R. M. Claramunt, C. López and J. Elguero, *J. Chem. Soc., Chem. Commun.*, 1994, 1143.
11 B. Beagley, K. J. Farnworth, E. T. Moss, R. G. Pritchard, S. Tajammal and A. E. Tipping, *Acta Crystallogr., Sect. C*, 1994, **50**, 1130.
12 A. L. Llamas-Saiz, C. Foces-Foces, I. Sobrados, J. Elguero and W. Meutermans, *Acta Crystallogr., Sect. C*, 1993, **49**, 724.
13 J. Elguero, N. Jagerovic, C. Foces-Foces, F. H. Cano, M. V. Roux, F. Aguilar-Parrilla and H.-H. Limbach, *J. Heterocycl. Chem.*, 1995, **32**, 451.
14 J. Berthou, J. Elguero and C. Rérat, *Acta Crystallogr., Sect. B*, 1970, **26**, 1880.
15 T. La Cour and S. E. Rasmussen, *Acta Chem. Scand.*, 1973, **27**, 1845.
16 C. Fontenas, C. Foces-Foces and J. Elguero, unpublished results.
17 C. Foces-Foces, F. H. Cano and J. Elguero, *Gazz. Chim. Ital.*, 1993, **123**, 477.
18 P. Domiano and A. Musati, *Cryst. Struct. Commun.*, 1974, **4**, 713.
19 H.-H. Limbach, *Dynamic NMR Spectroscopy in the Presence of Kinetic H/D Isotope Effects*, in *NMR Basic Principles and Progress*, Springer, Berlin, 1991.
20 H.-H. Limbach, G. Scherer, L. Meschede, F. Aguilar-Parrilla, B. Wehrle, J. Braun, Ch. Hoelger, H. Benedict, G. Buthowsky, W. P. Fehlhammer, J. Elguero, J. A. S. Smith and B. Chaudret, in *Ultrafast Reaction Dynamics and Solvent Effects*, eds. Y. Gauduel and P. J. Rossky, Am. Inst. Phys., New York, 1994, A.P. Conf. Proc. 258, pp. 225–239.
21 *Modern Techniques in Computational Chemistry: MOTECC-89*, ed. E. Clementi, ESCOM Science Publishers, Leiden, 1989.
22 *Modern Techniques in Computational Chemistry: MOTECC-90*, ed. E. Clementi, ESCOM Science Publishers, Leiden, 1990.
23 KGNMOL: R. Romperts and E. Clementi, IBM Technical Report KGN-118,119, 1988; QCPE 1988, **8** , 33, program 538; E. Clementi and G. Corongiu, in ch. 6 of ref. 21; E. Clementi, G. Corongiu and S. Chakravorty, in ch. 7 of ref. 22. KGNMOL is included in MOTECC code.
24 HONDO: M. Dupuis, J. Rys and H. F. King, *J. Chem. Phys.*, 1976, **65**, 111; HONDO7: M. Dupuis, J. D. Watts, G. J. B. Hurst and H. O. Villar, QCPE, 1987, program 544; HONDO8: M. Dupuis, P. Mourgenot, J. D. Watts, G. J. B. Hurst and H. O. Villar, in ch. 7 of ref. 22; A. Dupuis, A. Farazdel, S. P. Karna and S. A. Maluendes, in ch. 6 of ref. 23. HONDO8 is included in MOTECC code.
25 GAUSSIAN86, C. M. J. Frisch, J. S. Binkley, H. B. Schelegel, K. Raghavachari, C. F. Melius, P. L. Martin,J. J. P. Stewart, F. W. Bobrowitz, C. M. Rohlfing, L. R. Kahn, D. J. Defrees, R. Seeger, R. A. Whiteside, D. J. Fox, E. M. Fluder and J. A. Pople, Gaussian Inc., Pittsburg, PA, 1984.
26 W. J. Hehre, L. Radom, P. v. R. Schleyer and J. A. Pople, *Ab initio Molecular Orbital Theory*, Wiley, New York, 1986.
27 P. Van Duijneveldt, IBM Technical Report RJ-945, 1971. Contraction of the basis are described in L. Gianolio, R. Pavani and E. Clementi, *Gazz. Chim. Ital.*, 1978, **108**, 181 and in L. Gianolio and E. Clementi, *Gazz. Chim. Ital.*, 1980, **110**, 179.
28 C. Urdaneta, G. Corongiu and E. Clementi, IBM Technical Report KGN-133 (1987); E. Clementi and G. Corongiu, *Chem. Phys. Lett.*, 1982, **90**, 359 and IBM Technical Report POK-11 (1982).
29 T. H. Dunning and P. J. Hay, in *Methods of Electronic Theory Structure*, ed. H. E. Schaeffer III, Plenum Press, New York, 1977.
30 S. F. Boys and F. Bernardi, *Mol. Phys.*, 1970, **19**, 553.
31 J. A. Sordo, T. L. Sordo, G. M. Fernández, R. Gomperts, S. Chin and E. Clementi, *J. Chem. Phys.*, 1989, **90**, 6361.
32 O. Mó, J. L. G. de Paz and M. Yáñez, *Theor. Chim. Acta*, 1988, **73**, 307.
33 O. Mó, J. L. G. de Paz and M. Yáñez, *J. Phys. Chem.*, 1986, **90**, 5597.
34 D. Spangler, I. H. Williams and G. M. Maggiora, *J. Comput. Chem.*, 1983, **4**, 524.
35 B. A. Murtagh and R. W. H. Sargent, *Comput. J.*, 1970, **13**, 185; H. B. Schlegel, *J. Comput. Chem.*, 1984, **5**, 612.
36 C. Moller and M. S. Plesset, *Phys. Rev.*, 1934, **46**, 618. For implementation in KGNMOL see ref. 23; in HONDO see ref. 24, and in GAUSSIAN see ref. 26.
37 J. P. Perdew, *Phys. Rev. B*, 1986, **33**, 8822; J. Perdew and A. Zunger, *Phys. Rev. B*, 1981, **23**, 5048. For implementation in KGNMOL, see ref. 24.
38 J. L. Brédas, M. P. Poskin, J. Delhalle, J. M. André and H. Chojnaki, *J. Phys. Chem.*, 1984, **88**, 5882.
39 P. Ahlberg, K. Janné, S. Löfás. F. Nettelblad and L. Swahn, *J. Phys. Org. Chem.*, 1989, **2**, 429; P. Svensson, N. Å. Bergmann and P. Ahlberg, *J. Chem. Soc., Chem. Commun.*, 1990, 82; *Z. Naturforsch., Teil A*, 1989, **44**, 473; K. A. Nguyen, M. S. Gordon and D. G. Truhlar, *J. Am. Chem. Soc.*, 1991, **113**, 1596.
40 Y. Kim, *J. Am. Chem. Soc.*, 1996, **118**, 1522.
41 L. Jaroszewski, B. Lesyng, J. J. Tanner and J. A. McCammon, *Chem. Phys. Lett.*, 1990, **175**, 282.
42 L. Meschede and H.-H. Limbach, *J. Phys. Chem.*, 1991, **95**, 10267.
43 M. Perrin, A. Thozet, P. Cabildo, R. M. Claramunt, E.Valentin and J. Elguero, *Can. J. Chem.*, 1993, **71**, 1443.

Paper 6/03035A
Received 30*th April* 1996
Accepted 2*nd September* 1996